Thermodynamic Study on Phase Transition in Adsorbed Film of Fluoroalkanol at the Hexane/Water Interface. 4. Phase Transition in the Adsorbed Film of the Alkanol and Fluoroalkanol Mixture

Takanori Takiue,* Takehiko Matsuo, Norihiro Ikeda,† Kinsi Motomura, and Makoto Aratono

Department of Chemistry, Faculty of Science, Kyushu University 33, Fukuoka 812-8581, Japan

Received: November 21, 1997; In Final Form: April 6, 1998

The interfacial tension, γ, of the hexane solution of the 1-icosanol ($C_{20}OH$) and 1,1,2,2-tetrahydroheptadecafluorodecanol ($FC_{10}OH$) mixture against water was measured as a function of total molality m and composition of $FC_{10}OH$, X_2, at 298.15 K under atmospheric pressure. All the γ vs m curves have a break point (first break) that corresponds to the phase transition from the expanded to the condensed state. Furthermore, it was found that the curves at $X_2 = 0.275$ and 0.280 show another break (second break) at a high concentration. By calculating the interfacial density Γ^H and then drawing the interfacial pressure, π, vs area per adsorbed molecule, A, curves, it was suggested that the first-order phase transition takes place from the expanded to the condensed film of $C_{20}OH$ at $X_2 < 0.250$ and to that of $FC_{10}OH$ at $X_2 > 0.300$ at the first break point. Furthermore the second break point was suggested to correspond to the first-order phase transition from the $FC_{10}OH$ condensed film to the $C_{20}OH$ condensed film. These findings were confirmed by the interfacial densities of individual components and support that $C_{20}OH$ and $FC_{10}OH$ molecules are completely immiscible in the condensed film, although they are miscible with each other at all proportions in the expanded film. Furthermore, it is shown that the phase transition from the $C_{20}OH$ to the $FC_{10}OH$ condensed state does not take place at the second break point because the cross-sectional area of the fluorocarbon chain is larger than that of the hydrocarbon chain and the condensed film is constructed of individual alcohol molecules.

Introduction

It is well-known that the mutual interaction between hydrocarbon and fluorocarbon chains is very weak, and therefore some of the mixtures of hydrocarbon and fluorocarbon surfactants are demixed in the micelle.[1−7] In the recent studies on the adsorption of such mixtures from their aqueous solutions,[8−10] we have found that these water-soluble surfactants are miscible with each other at all proportions in the adsorbed films at their aqueous solution/oil (or air) interfaces even when they are partially miscible within a limited composition in the micelle. Therefore, it is of great interest to investigate the adsorption of an oil-soluble mixture of fluorocarbon and hydrocarbon compounds at the water/oil solution interface.

Keeping in mind that the phase transition in the adsorbed film is influenced appreciably by molecular interaction and both long-chain hydrocarbon and fluorocarbon alcohols are soluble only in oil and exhibit phase transition,[11−16] we employed the 1,1,2,2-tetrahydroheptadecafluorodecanol ($FC_{10}OH$) and 1-icosanol ($C_{20}OH$) mixture. This combination was selected because the same kind of phase transition between the expanded and the condensed states has been observed for the pure $FC_{10}OH$ system[14,16] and is expected for the pure $C_{20}OH$ system,[11,12] and their individual adsorption behavior at the hexane/water interface was clarified through our systematic thermodynamic studies.[11−16] In this paper, we will focus on the phase transition in the adsorbed film of the $C_{20}OH$ and $FC_{10}OH$ mixture.

The interfacial tension γ of the hexane solution of this mixture against water was measured as a function of total molality m and composition of $FC_{10}OH$, X_2, at 298.15 K under atmospheric pressure. The total interfacial density Γ^H was evaluated, and the interfacial pressure, π, vs mean area per adsorbed molecule, A, curves were drawn to make clear the state of the adsorbed film.

Experimental Section

1-Icosanol ($C_{20}OH$) purchased from Sigma Ltd. was recrystallized seven times from hexane. The purity of $C_{20}OH$ was checked by gas−liquid chromatography and by observing no time dependence of interfacial tension between its hexane solution and water. The purification of 1,1,2,2-tetrahydroheptadecafluorodecanol ($FC_{10}OH$) was described previously.[14] Water was distilled three times from dilute alkaline permanganate solution and hexane once in the presence of metallic sodium particles. Their purity was checked by measuring the interfacial tension between them.

The interfacial tension was measured by the pendant drop method[17] within an experimental error of 0.05 mN m^{-1}. The densities of pure hexane and water[18,19] were used instead of those of hexane solution and water because of a sufficiently low concentration of the hexane solution and negligibly small mutual solubility between them.

Results and Discussion

The interfacial tension, γ, of the hexane solution of a $C_{20}OH$ and $FC_{10}OH$ mixture against water was measured as a function

* To whom correspondence should be addressed.

† Present address: Department of Environmental Science, Faculty of Human Environmental Science, Fukuoka Women's University, Fukuoka 813-8529, Japan.

S1089-5647(98)00292-2 CCC: $15.00
Published on Web 05/28/1998

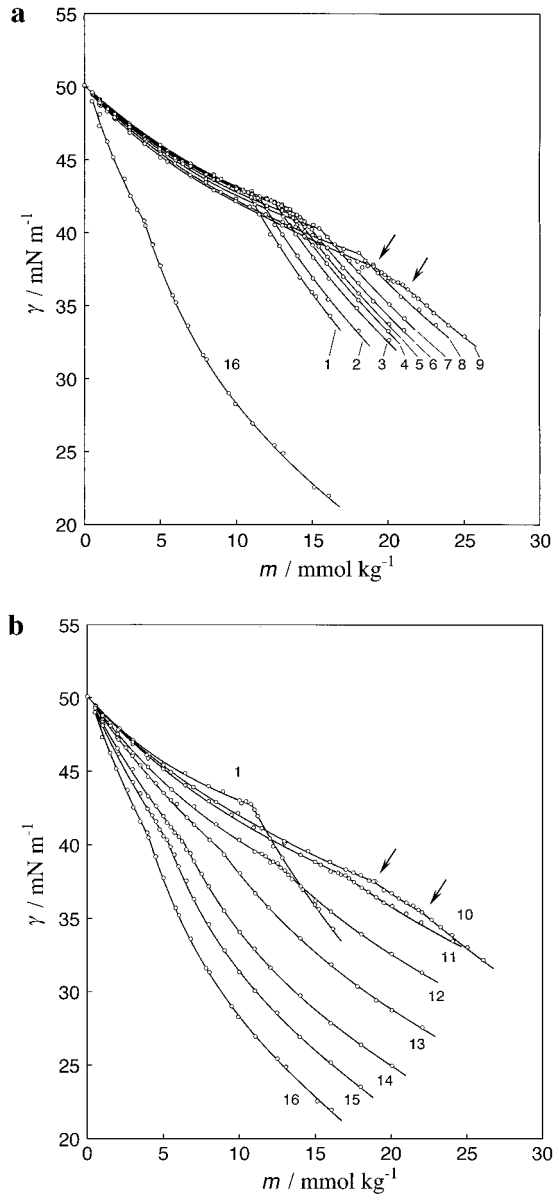

Figure 1. (a) Interfacial tension vs total molality curves at constant composition: X_2 = (1) 0, (2) 0.050, (3) 0.100, (4) 0.125, (5) 0.150, (6) 0.170, (7) 0.200, (8) 0.250, (9) 0.275, (16) 1. (b) Interfacial tension vs total molality curves at constant composition: X_2 = (1) 0, (10) 0.280, (11) 0.300, (12) 0.375, (13) 0.500, (14) 0.650, (15) 0.800, (16) 1.

of total molality m and composition of $FC_{10}OH$ X_2 defined by

$$m = m_1 + m_2 \tag{1}$$

and

$$X_2 = m_2/m \tag{2}$$

at 298.15 K under atmospheric pressure. Here m_1 and m_2 are the molalities of $C_{20}OH$ and $FC_{10}OH$, respectively. The γ value was plotted against m at constant composition in Figure 1. The γ vs m curves at compositions below 0.275 are shown in Figure 1a and those above 0.280 in Figure 1b together with those at X_2 = 0 and 1. It is seen that the γ value decreases with increasing concentration, and all the curves have a distinct break point at which the slope of the curve changes abruptly. It should be noted that the two break points were observed on the curves at X_2 = 0.275 and 0.280 as shown by the arrows. These breaks

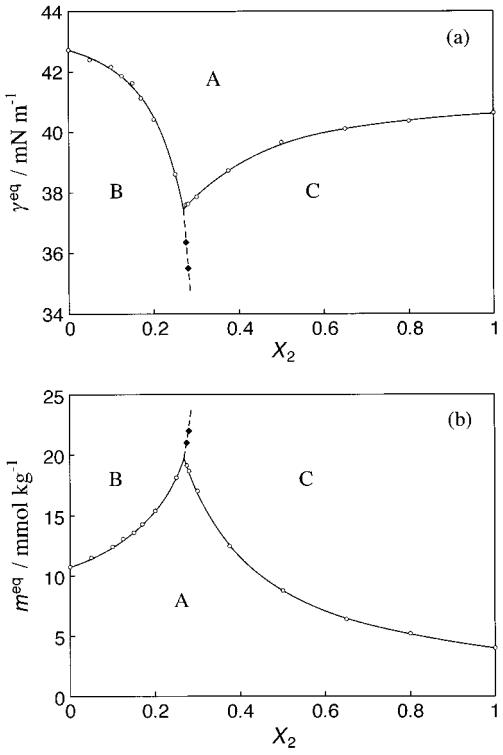

Figure 2. (a) Equilibrium interfacial tension vs composition curves: (○) first break point, (◆) second break point. (b) Equilibrium total molality vs composition curves: (○) first break point, (◆) second break point.

of the γ vs m curves suggest that one or two kinds of phase transitions take place in the adsorbed film of the $C_{20}OH$ and $FC_{10}OH$ mixture at the hexane/water interface. Here let us call the break point at a higher concentration observed at X_2 = 0.275 and 0.280 the second break point and the others the first one.

The interfacial tension γ^{eq} and the total molality m^{eq} of the break points are plotted against bulk composition X_2 in Figure 2. It is seen that the γ^{eq} vs X_2 curve of the first break point has a sharp-pointed minimum, and the corresponding m^{eq} vs X_2 curve has a sharp-pointed maximum; the addition of one component to the other causes an increase in m^{eq} and a decrease in γ^{eq}, respectively. Furthermore, the γ^{eq} and m^{eq} vs X_2 curves of the second break point touch the curves of the first break point at the cusp. Therefore this figure implies that there exist three different states (shown by A, B, and C) in the adsorbed film of the $C_{20}OH$ and $FC_{10}OH$ mixture. It is noted that the γ^{eq} value of the second break point decreases and the corresponding m^{eq} value increases very steeply with increasing X_2.

Now let us summarize briefly the thermodynamic relations for analyzing the experimental results. Since the mixture employed in this study is the nonionic−nonionic one, the fundamental equation describing the interfacial tension is given by[20]

$$d\gamma = -s^H\, dT + v^H\, dp - \Gamma_1^H\, d\mu_1 - \Gamma_2^H\, d\mu_2 \tag{3}$$

where s^H, v^H, and Γ_i^H are the interfacial excess entropy, volume, and the number of moles of solute i per unit area defined with respect to the two dividing planes which make the excess number of moles of water and hexane zero, respectively. By assuming the hexane solution to be ideally dilute and substituting the total differential of chemical potential

of component i, μ_i, into eq 3, we have

$$d\gamma = -\Delta s\, dT + \Delta v\, dp - (\Gamma_1^H RT/m_1)dm_1 - (\Gamma_2^H RT/m_2)dm_2 \quad (4)$$

where Δy is the thermodynamic quantity change associated with adsorption of alcohols from their hexane solution given by

$$\Delta y = y^H - \Gamma_1^H y_1 - \Gamma_2^H y_2, \quad y = s \text{ and } v \quad (5)$$

Equation 4 shows that the Γ_1^H and Γ_2^H values are evaluated separately by measuring the dependence of interfacial tension on m_1 at constant m_2 and on m_2 at constant m_1, respectively. This is one way to elucidate the interfacial behavior of the system. Another way is to adopt m and X_2, instead of m_1 and m_2, as independent variables. In this case eq 4 is rewritten as

$$d\gamma = -\Delta s\, dT + \Delta v\, dp - (\Gamma^H RT/m)dm - (\Gamma^H RT/X_1X_2)(X_2^H - X_2)dX_2 \quad (6)$$

Therefore, the total interfacial density Γ^H and the composition of the adsorbed film X_2^H, defined respectively by

$$\Gamma^H = \Gamma_1^H + \Gamma_2^H \quad (7)$$

and

$$X_2^H = \Gamma_2^H/\Gamma^H \quad (8)$$

are evaluated separately by measuring the interfacial tension as a function of m and X_2.[20] Since our goal of the series of this study is to construct the m vs X_2 and X_2^H diagram (phase diagram of adsorption) and to clarify the miscibility of alcohols in the adsorbed film on the basis of the diagram from the viewpoint of the molecular interaction[21] over a whole composition range from pure $C_{20}OH$ ($X_2 = 0$) to $FC_{10}OH$ ($X_2 = 1$), we adopted the independent variables m and X_2^H.

First, we evaluated the total interfacial density by applying the equation obtained from eq 6,

$$\Gamma^H = -(m/RT)(\partial\gamma/\partial m)_{T,p,X_2} \quad (9)$$

to the γ vs m curves in Figure 1. The results are shown as the Γ^H vs m curves at constant X_2 in Figure 3. It is seen that the Γ^H value increases with increasing m and changes discontinuously at a concentration corresponding to the break point on the γ vs m curve. It should be noted that the Γ^H value converges at about 8 μmol m^{-2} below $X_2 = 0.250$ (Figure 3a) and at about 5 μmol m^{-2} above $X_2 = 0.300$ (Figure 3b) at high concentrations. Furthermore, it is seen that the Γ^H vs m curves at $X_2 = 0.275$ and 0.280 consist of three parts connected by two discontinuous changes; the Γ^H value is about 5 and 8 μmol m^{-2} just after the first and the second break points, respectively. Therefore, it is said that there are three different states of adsorbed film depending on the bulk composition and total molality.

To make clear the state of the adsorbed film, we first calculated the interfacial pressure π and the mean area per adsorbed molecule A values by

$$\pi = \gamma^0 - \gamma \quad (10)$$

and

$$A = 1/N_A\Gamma^H \quad (11)$$

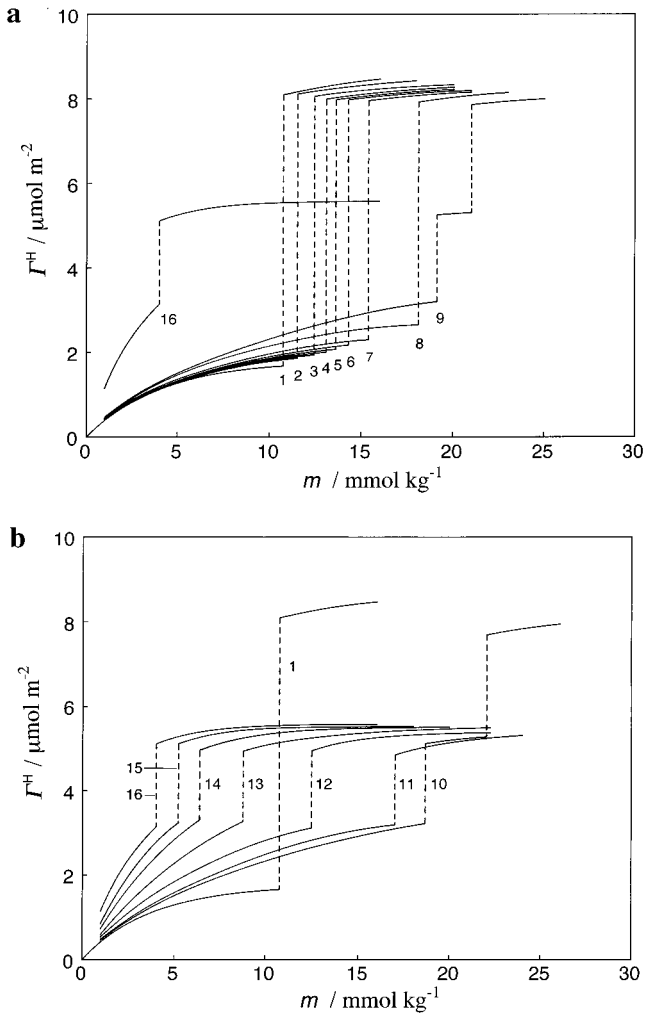

Figure 3. (a) Total interfacial density vs total molality curves at constant composition: X_2 = (1) 0, (2) 0.050, (3) 0.100, (4) 0.125, (5) 0.150, (6) 0.170, (7) 0.200, (8) 0.250, (9) 0.275, (16) 1. (b) Total interfacial density vs total molality curves at constant composition: X_2 = (1) 0, (10) 0.280, (11) 0.300, (12) 0.375, (13) 0.500, (14) 0.650, (15) 0.800, (16) 1.

where γ^0 is the interfacial tension of the pure hexane/water interface and N_A is Avogadro's number, and then drew the π vs A curves at constant composition in Figure 4. It is seen from Figure 4a,b that the π vs A curves consist of two parts connected by one discontinuous change. The one shows a gradual increase in π and the other a very steep increase with decreasing A. It is found that the A value of the latter state converges at about 0.2 nm^2 below $X_2 = 0.250$ and 0.3 nm^2 above $X_2 = 0.300$. Taking account of our previous findings[11,14] that the adsorbed film of $FC_{10}OH$ and that of 1-octadecanol ($C_{18}OH$), which is an analogue of $C_{20}OH$ with a shorter chain, exhibit a phase transition between the expanded and the condensed states and that the A values of their condensed states are very close to the values of the cross-sectional area of their hydrophobic chains, we concluded that the phase transition takes place from the expanded to the condensed state at the first break point. Furthermore, the convergence of A at the two different values suggests that the condensed film is constructed of $C_{20}OH$ molecules at $X_2 < 0.250$ and $FC_{10}OH$ at $X_2 > 0.300$. Deducing from the fact that the cross-sectional area of hydrophobic chains of these alcohols is larger than that of their hydroxyl group and therefore the A value of the condensed state is determined by the size of hydrophobic chain, we assume that the packing of molecules in the condensed state is hexagonal with vertical

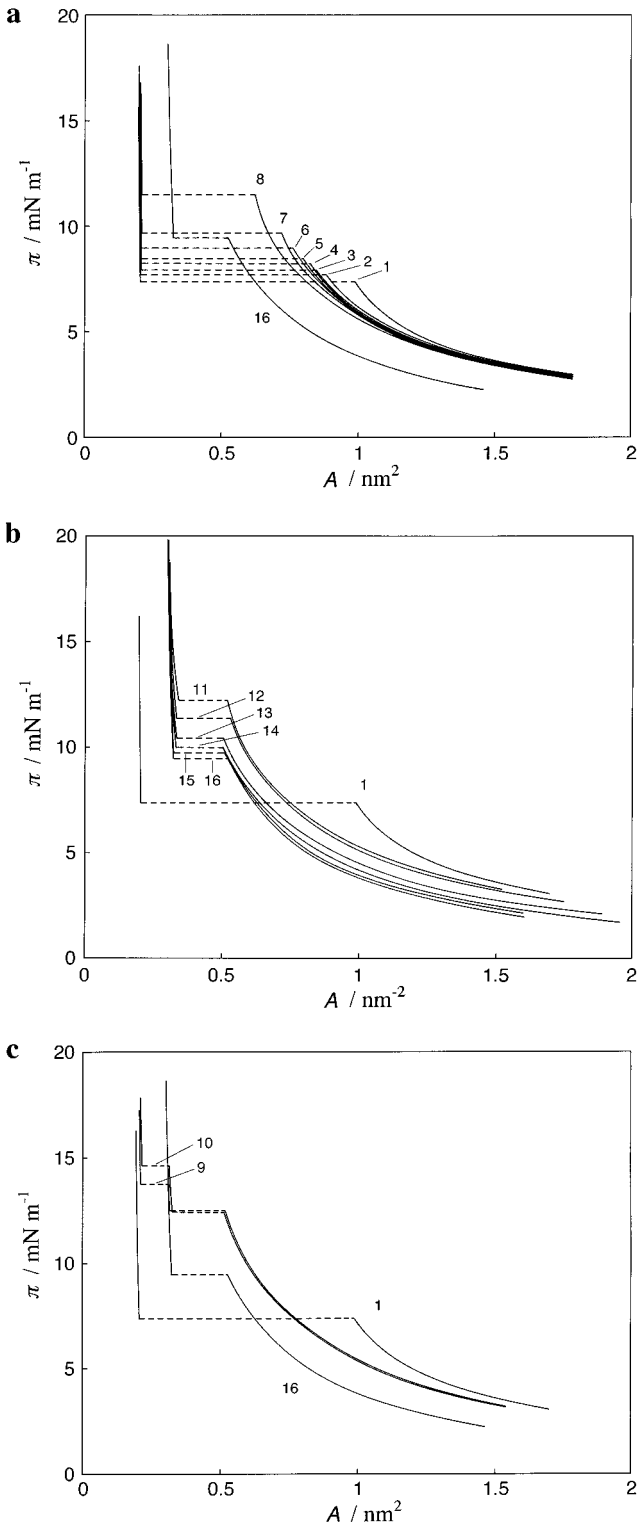

Figure 4. (a) Interfacial pressure vs area per adsorbed molecule curves at constant composition: X_2 = (1) 0, (2) 0.050, (3) 0.100, (4) 0.125, (5) 0.150, (6) 0.170, (7) 0.200, (8) 0.250, (16) 1. (b) Interfacial pressure vs area per adsorbed molecule curves at constant composition: X_2 = (1) 0, (11) 0.300, (12) 0.375, (13) 0.500, (14) 0.650, (15) 0.800, (16) 1. (c) Interfacial pressure vs area per adsorbed molecule curves at constant composition: X_2 = (1) 0, (9) 0.275, (10) 0.280, (16) 1.

orientation at the interface. This may be clarified by observing the film with X-ray or neutron reflection[22,23] and diffraction[24,25] if these techniques are applicable to the adsorbed film at the oil/water interface. On the other hand, since the A value of the expanded state varies continuously with bulk composition, the film is constructed by the $C_{20}OH$ and $FC_{10}OH$ mixtures and the molecular packing is relatively loose.

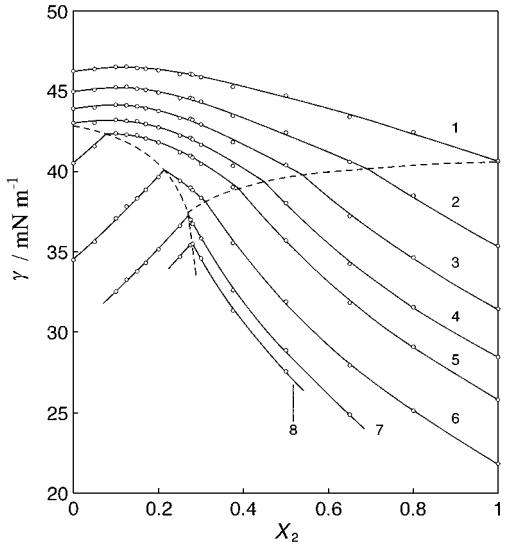

Figure 5. Interfacial tension vs composition curves at constant total molality: m = (1) 4, (2) 6, (3) 8, (4) 10, (5) 12, (6) 16, (7) 20, (8) 22 mmol kg^{-1}; (- - -) γ^{eq} vs X_2.

In Figure 4c are shown the π vs A curves at $X_2 = 0.275$ and 0.280 together with the curves of pure alcohols. It is seen that the curves consist of two discontinuous changes among three different states. By comparing the curves at 0.275 and 0.280 with those of pure alcohols, we can say that the first transition corresponds to the one from the expanded to the condensed film of $FC_{10}OH$ and the second to the one from the condensed film of $FC_{10}OH$ to that of $C_{20}OH$. Now summarizing the results of the π vs A curves and looking at Figure 2 again, it is concluded that the three regions A, B, and C correspond to the expanded, $C_{20}OH$ condensed, and $FC_{10}OH$ condensed state, respectively.

The interfacial density of $C_{20}OH$, Γ_1^H, and that of $FC_{10}OH$, Γ_2^H, may confirm this conclusion. As mentioned above, the direct way to evaluate the interfacial densities of individual components is to apply eq 4 to the γ vs m_1 and m_2 curves. However, for evaluating them from our experimental results, we first illustrated the γ vs X_2 curve at a given m in Figure 5 and then calculated the interfacial densities of individual components by using the equations

$$\Gamma_1^H = X_1\Gamma^H + (X_1X_2/RT)(\partial\gamma/\partial X_2)_{T,p,m} \qquad (12)$$

and

$$\Gamma_2^H = X_2\Gamma^H - (X_1X_2/RT)(\partial\gamma/\partial X_2)_{T,p,m} \qquad (13)$$

which are derived from eqs 6 and 7. It is seen from Figure 5 that the γ vs X_2 curve at a low concentration has a rounded maximum and that at a high concentration has a sharp-pointed maximum. At an intermediate concentration, the curve shows one or two breaks on the γ^{eq} vs X_2 curves.

Figure 6 shows the interfacial densities (Γ_1^H, Γ_2^H, and Γ^H) vs X_2 curves at $m = 4$ and 20 mmol kg^{-1}. It is noted that curve 1 at 4 mmol kg^{-1} in Figure 5 is in the expanded state region and that the individual Γ_i^H and therefore Γ^H values change gradually with increasing X_2. On the other hand, curve 7 at 20 mmol kg^{-1} in Figure 5 is in the two different condensed states region, and the interfacial densities change discontinuously at about $X_2 = 0.270$. It is important to note that the Γ^H value below $X_2 = 0.270$ is very close to Γ_1^H and that above to Γ_2^H,

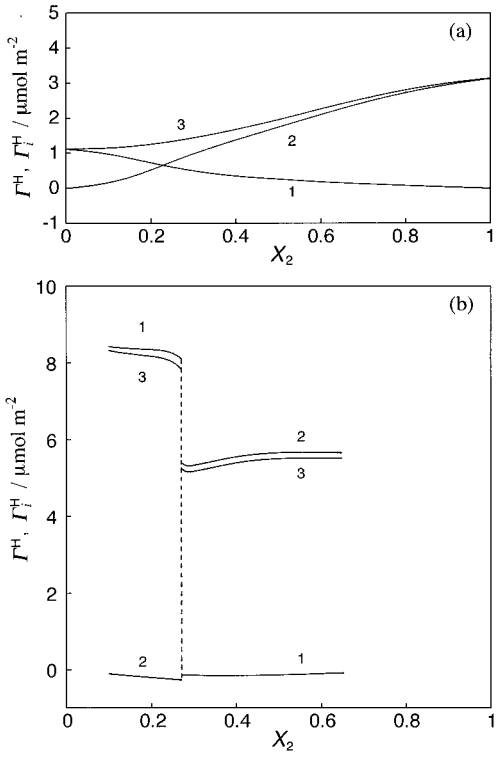

Figure 6. Interfacial density vs composition curves at constant total moloality: (a) $m = 4$ mmol kg^{-1}, (b) $m = 20$ mmol kg^{-1}; (1) Γ_1^H vs X_2, (2) Γ_2^H vs X_2, (3) Γ^H vs X_2.

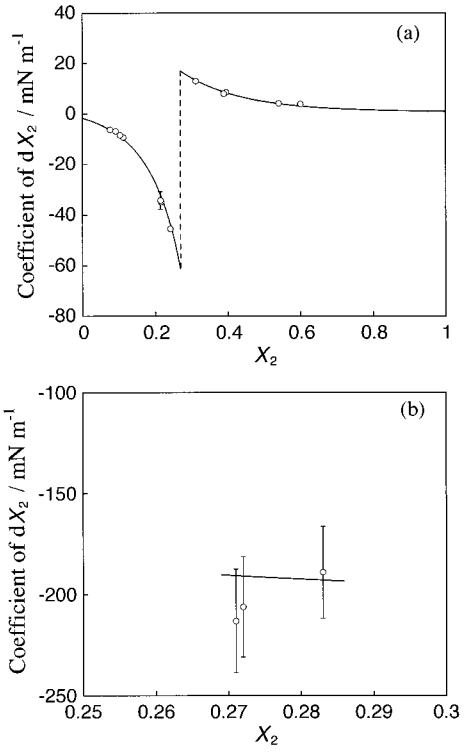

Figure 7. (a) Values of coefficient of dX_2 of eqs 16 and 17 vs composition curve for the first break point: (○) eq 16, (—) eq 17. (b) Values of coefficient of dX_2 of eqs 16 and 17 vs composition curve for the second break point: (○) eq 16, (—) eq 17.

respectively. This result confirms our deduction that the condensed film is constructed from $FC_{10}OH$ or $C_{20}OH$ molecules, which depends on m and X_2, and therefore $FC_{10}OH$ and $C_{20}OH$ molecules are practically immiscible in the condensed state because of the very weak mutual interaction between them. The miscibility of $C_{20}OH$ and $FC_{10}OH$ in the adsorbed film will be discussed in detail by evaluating the composition of the adsorbed film X_2^H value and drawing the phase diagram of adsorption in the next paper.[21]

Next, we briefly mention the order of phase transitions found in this study. When the two states α and β coexist in the adsorbed film, the following equations hold simultaneously:

$$d\gamma^{eq} = -\Delta s^{\alpha}\, dT + \Delta v^{\alpha}\, dp - (\Gamma^{H,\alpha}RT/m^{eq})dm^{eq} - (\Gamma^{H,\alpha}RT/X_1X_2)(X_2^{H,\alpha} - X_2)dX_2 \quad (14)$$

and

$$d\gamma^{eq} = -\Delta s^{\beta}\, dT + \Delta v^{\beta}\, dp - (\Gamma^{H,\beta}RT/m^{eq})dm^{eq} - (\Gamma^{H,\beta}RT/X_1X_2)(X_2^{H,\beta} - X_2)dX_2 \quad (15)$$

By eliminating dm^{eq} from these equations, the interfacial tension at the break point γ^{eq} is given as a function of T, p, and X_2 by

$$d\gamma^{eq} = -[(\Delta s^{\beta}/\Gamma^{H,\beta} - \Delta s^{\alpha}/\Gamma^{H,\alpha})/(1/\Gamma^{H,\beta} - 1/\Gamma^{H,\alpha})]dT + [(\Delta v^{\beta}/\Gamma^{H,\beta} - \Delta v^{\alpha}/\Gamma^{H,\alpha})/(1/\Gamma^{H,\beta} - 1/\Gamma^{H,\alpha})]dp - [(RT/X_1X_2)(X_2^{H,\beta} - X_2^{H,\alpha})/(1/\Gamma^{H,\beta} - 1/\Gamma^{H,\alpha})]dX_2 \quad (16)$$

γ^{eq} is also written in a differential form as

$$d\gamma^{eq} = (\partial\gamma^{eq}/\partial T)_{p,X_2}dT + (\partial\gamma^{eq}/\partial p)_{T,X_2}dp + (\partial\gamma^{eq}/\partial X_2)_{T,p}\, dX_2 \quad (17)$$

Here the $(\partial\gamma^{eq}/\partial X_2)_{T,p}$ value in eq 17 was obtained from the slope of the γ^{eq} vs X_2 curves shown in Figure 2a. The coefficient of dX_2 in eq 16 was calculated as follows; at first the $\Gamma_i^{H,\alpha}$ and $\Gamma_i^{H,\beta}$ values were obtained by extrapolating the Γ_i^H vs X_2 curve at a given m shown in Figure 6b to the phase transition points, and then the values of $\Gamma^{H,\alpha}$ and $X_2^{H,\alpha}$ and the corresponding quantities for the β state calculated by using eqs 7 and 8 were substituted into eq 16 to give the values of coefficient of dX_2. In Figure 7 the coefficient of dX_2 of eq 16 is compared with that of eq 17. It is seen that the agreement is fairly good within experimental error for both transitions, and therefore it is probable that the first-order phase transition takes place in the adsorbed film of the $C_{20}OH$ and $FC_{10}OH$ mixture at the hexane/water interface.

Finally, let us examine the phase transition in the special case that the two components are completely immiscible in the α and β states, e.g., the α state is constructed by the second component ($X_2^{H,\alpha} \approx 1$) and the β by the first component ($X_2^{H,\beta} \approx 0$). The dependence of γ^{eq} on X_2 is derived from eq 16 and reduced to

$$(\partial\gamma^{eq}/\partial X_2)_{T,p} = (RT/X_1X_2)/(1/\Gamma_1^{H,\beta} - 1/\Gamma_2^{H,\alpha}) \quad (18)$$

for the special case. Here $\Gamma^{H,\alpha}$ and $\Gamma^{H,\beta}$ are written by $\Gamma_2^{H,\alpha}$ and $\Gamma_1^{H,\beta}$, respectively, because it is assumed that $X_2^{H,\alpha} = 1$ and $X_2^{H,\beta} = 0$. Then eq 18 shows that the sign of $(\partial\gamma^{eq}/\partial X_2)_{T,p}$ is determined only by the inequality between $\Gamma_1^{H,\beta}$ and $\Gamma_2^{H,\alpha}$. Let us assume $\Gamma_1^{H,\beta} > \Gamma_2^{H,\alpha}$. Therefore $(\partial\gamma^{eq}/\partial X_2)_{T,p}$ should be negative. Taking into account that the film state is α for the larger X_2 value, the negative $(\partial\gamma^{eq}/\partial X_2)_{T,p}$ means that the phase transition should take place from the α state having the smaller interfacial density to the β having the larger one as the γ value of the mixture is decreased. Similarly the composition depen-

dence of m^{eq} is given from eqs 14 and 15 by

$$(\partial m^{eq}/\partial X_2)_{T,p} = (m^{eq}/X_1X_2)[X_2 + \Gamma_2^{H,\alpha}/(\Gamma_1^{H,\beta} - \Gamma_2^{H,\alpha})] \quad (19)$$

for the special case when the two components are completely immiscible in the two states. With respect to the present system, Figure 3 shows that the interfacial density of the condensed film of $FC_{10}OH$, $\Gamma_2^{H,\alpha}$, is smaller than that of $C_{20}OH$, $\Gamma_1^{H,\beta}$. Then $(\partial m^{eq}/\partial X_2)_{T,p}$ should be positive and the phase transition should take place from the $FC_{10}OH$ condensed state to the C_{20}-OH condensed state as the total molality is increased. Figure 2 proves this situation: $(\partial \gamma^{eq}/\partial X_2)_{T,p}$ is negative and $(\partial m^{eq}/\partial X_2)_{T,p}$ is positive. Therefore the phase transition takes place from the $FC_{10}OH$ condensed state to the $C_{20}OH$ condensed state, but its reverse does not take place.

Acknowledgment. This work was supported in part by The Grant for Physics and Chemistry Reasearch from Shiseido Co., Ltd., and in part by Kurata Foundation.

References and Notes

(1) Mukerjee, P.; Yang, A. Y. S. *J. Phys. Chem.* **1976**, *80*, 1388.
(2) Shinoda, K.; Nomura, T. *J. Phys. Chem.* **1980**, *84*, 365.
(3) Funasaki, N.; Hada, S. *J. Phys. Chem.* **1980**, *84*, 736.
(4) Haegel, F. H.; Hoffmann, H. *Prog. Colloid Polym. Sci.* **1988**, *76*, 132.
(5) Asakawa, T.; Mouri, M.; Miyagishi, S.; Nishida, M. *Langmuir* **1989**, *5*, 343.
(6) Clapperton, R. M.; Ottewill, R. H.; Ingram, B. T. *Langmuir* **1994**, *10*, 51.
(7) *Fluorinated Surfactants*; Kissa, E., Ed.; Marcel Dekker: New York, 1994; Chapter 7.
(8) Matsuki, H.; Ikeda, N.; Aratono, M.; Kaneshina, S.; Motomura, K. *J. Colloid Interface Sci.* **1992**, *150*, 331.
(9) Matsuki, H.; Ikeda, N.; Aratono, M.; Kaneshina, S.; Motomura, K. *J. Colloid Interface Sci.* **1992**, *154*, 454.
(10) Aratono, M.; Ikeguchi, M.; Takiue, T.; Ikeda, N.; Motomura, K *J. Colloid Interface Sci.* **1995**, *174*, 156.
(11) Matubayasi, N.; Motomura, K.; Aratono, M.; Matuura, R. *Bull. Chem. Soc. Jpn.* **1978**, *51*, 2800.
(12) Ikenaga, T.; Matubayasi, N.; Aratono, M.; Motomura, K.; Matuura, R. *Bull. Chem. Soc. Jpn.* **1980**, *53*, 653.
(13) Hayami, Y.; Uemura, A.; Ikeda, N.; Aratono, M., Motomura, K. *J. Colloid Interface Sci.* **1995**, *172*, 142.
(14) Takiue, T.; Yanata, A.; Ikeda, N.; Motomura, K.; Aratono, M. *J. Phys. Chem.* **1996**, *100*, 13743.
(15) Takiue, T.; Yanata, A.; Hayami, Y.; Ikeda, N.; Motomura, K.; Aratono, M. *J. Phys. Chem.* **1996**, *100*, 20122.
(16) Takiue, T.; Uemura, A.; Ikeda, N.; Motomura, K.; Aratono, M. *J. Phys. Chem. B*, in press.
(17) Matubayasi, N.; Motomura, K.; Kaneshina, S.; Nakamura, M.; Matuura, R. *Bull. Chem. Soc. Jpn.* **1977**, *50*, 523.
(18) Kell, G. S.; Whally, E. *Philos. Trans. R. Soc. London A* **1965**, *258*, 565.
(19) Orwoll, R. A.; Flory, P. J. *J. Am. Chem. Soc.* **1967**, *89*, 6814.
(20) Motomura, K.; Aratono, M. In *Mixed Surfactant Systems*; Ogino, K., Abe, M., Eds.; Marcel Dekker: New York, 1993; Vol. 46, p 99.
(21) Takiue, T.; Matsuo, T.; Ikeda, N.; Motomura, K.; Aratono, M. *J. Phys. Chem. B*, submitted for publication.
(22) Doerr, A.; Wu, X. Z.; Ocko, B. M.; Sirota, E. B.; Gang, O.; Deutsch, M. *Colloids Surf. A* **1997**, *128*, 63.
(23) Li, Z. X.; Lu, J. R.; Thomas, R. K.; Rennie, A. R.; Penfold, J. *J. Chem. Soc., Faraday Trans.* **1996**, *92*, 565.
(24) Renault, A.; Legrand, J. F.; Goldmann, M.; Berge, B. *J. Phys. II Fr.* **1993**, *3*, 761.
(25) Brezesinski, G.; Scalas, E.; Struth, B.; Möhwald, H.; Bringezu, F.; Gehlert, U.; Weidemann, G.; Vollhardt, D. *J. Phys. Chem.* **1995**, *99*, 8758.